# Enabling Technologies for Compact Integrated Electric Drives for Automotive Traction Applications

Shajjad Chowdhury, Emre Gurpinar, Gui-Jia Su, Tsarafidy Raminosoa, Timothy A. Burress, and Burak Ozpineci Power Electronics and Electric Machinery Group Oak Ridge National Laboratory Knoxville, TN 37932 chowdhuryms@ornl.gov

Abstract— The electric traction drive is the main consumer of the stored energy in an electric vehicle. Therefore, the drive system must perform with high efficiency to maximize the vehicle range for given battery capacity. Since the introduction of hybrid electric vehicles, various innovative traction drive technologies have been implemented in commercially available electric vehicles to increase efficiency and power density. It is expected that the power density and performance of the traction drive unit must improve significantly for future electric vehicles to increase the user space in the vehicle, extend the range and increase market adoption. US Department of Energy (DOE) has recently announced technical targets for light duty electric vehicles. DOE targets to reach a power density target of 33 kW/L for a 100 kW traction drive system by 2025. It is an increment by a factor of 5.5 in comparison to the state-of-the-art. This paper investigates the current trends in commercially available electric drives for light-duty automotive applications, identifies the challenges, and discusses innovative technologies to overcome the power density barrier.

Keywords—Automotive traction application, electric traction drive, integrated motor drive.

#### I. INTRODUCTION

vehicles have experienced significant improvements in the past decade with the introduction of hybrid and plugin hybrid versions of the popular gasolinebased models, followed by battery electric (BEV) models. Some of the BEVs in the market can travel more than 300 miles with a full charge [1]. Furthermore, these vehicles take advantage of high torque capability of electric motors at low speed and provide high performance in comparison to combustion engines. These two factors are slowly increasing the market acceptance of the electric vehicles by overcoming range anxiety and providing high performance. Department of Energy (DOE), Vehicle Technology Office (VTO) has announced 2025 technical targets for electric drive components in U.S. Drive Electrical and Electronics Technical Team (EETT) Roadmap [2] to support the mass market adoption of electric vehicles.

This manuscript has been authored by UT-Battelle, LLC, under Contract No. DE-AC0500OR22725 with the U.S. Department of Energy. The United States Government retains and the publisher, by accepting the article for publication, acknowledges that the United States Government retains a nonexclusive, paid-up, irrevocable, world-wide license to publish or reproduce the published form of this manuscript, or allow others to do so, for the United States Government purposes. The Department of Energy will provide public access to these results of federally sponsored research in accordance with the DOE Public Access Plan (http://energy.gov/downloads/doe-public-accessplan).

Technical guideline in the roadmap has set the goal to increase power handling capability by almost two times (55 kW to 100 kW). Furthermore, the power density target for the power electronics is set to increase 5.6 times (18 kW/L to 100 kW/L), which requires advanced integration of the power module with a reduced footprint (e.g. reduced electrical parasitic and increased thermal performance). The power density target of the traction motor has also increased from 9 kW/L to 50 kW/L. Finally, the target for the system power density is expected to increase 5.5 times (6 kW/L to 33 kW/L) for 100 kW system by 2025, in comparison with on-road vehicle status.

The objective of this paper is to provide an overview of electric drive technologies adopted by the automotive industry. Several commercialized electric drive systems have been analyzed and compared including a detailed analysis of power electronics and electric motor topologies, and power modules to identify the state-of-the-art in commercial vehicles and opportunities for future improvements. Finally, several technologies have been discussed that can lead to the DOE 2025 power density target.

# II. ELECTRIC DRIVE IN AUTOMOTIVE TRACTION APPLICATION

The requirements for an electric drive for traction applications are very demanding in terms of efficiency, power density, and cost. Over the years, vehicle manufacturers employed various technologies to achieve high efficiency and power dense solution. Oak Ridge National Laboratory (ORNL) has been working towards understanding these commercialized electric vehicle technologies. A few of the analyzed electric drive system specifications and power densities are summarized in Table I. Power ratings shown in Table I are not always continuous power, only Nissan Leaf has the continuous capability near the rated power. It can be seen from the table that the drive system of the 2014 Honda Accord and 2016 BMW i3 have the highest power density and both can deliver up to 125kW of peak power [3]. These power ratings are close to the power rating targeted in the 2025 roadmap [2]. A three-phase permanent magnet synchronous motor (PMSM) has been used for both vehicles to achieve high power density.

These motor units are driven by a three-phase two-level IGBT based inverter. The EV manufacturers widely adopt this two-level inverter topology and the semiconductor technology due to its simplicity and robustness. A picture of the motor and the inverter of these two electric drive units are shown in Fig. 1(a-b). An experimental efficiency map is

also shown in Fig. 1, it can be seen that both the traction drive systems can achieve up to 94% efficiency [3]. These two drive units utilize different DC link voltages, BMW i3 has 355V DC bus with the combined capacitance of 475 $\mu$ F. Honda Accord utilized a much higher voltage of 700V thus only two parallel semiconductor devices per switch is used rather than four in BMW i3 [3, 4]. On the other hand, Honda Accord requires much higher energy storage due to the additional boost converter. It uses  $1225\mu$ F capacitance to stabilize the DC link voltage. In both cases, a film capacitor is used due to its reliability, high energy density, and self-healing capability.

In recent years, EV manufacturers are putting more effort into improving the power density of the electric drive unit. This is easily noticeable from the design trend of Toyota

Prius electric drive systems. The first-generation Prius entered the automotive market in 1997. They used a threephase PM motor with a single magnet arrangement for the motor driven by an inverter with an input DC link voltage of 275V [5, 6]. The machine was designed to operate at 6000 rpm leading to lower overall power density than 2017 Toyota Prius. The design trend in Prius is shown in Fig. 1(c) where it can be noticed that the DC bus voltage has increased from 375V to 600V/650V over the years while the motor speed has ramped up from 6000 rpm to 17000 rpm; thus, the size of the motor and inverter has been reduced [4, 5, 7-9]. The magnet arrangement in the rotor assembly has also changed from a single to double V shape in the second-generation Prius. The third-generation rotors include three magnets per pole to increase the reluctance torque and to improve the high-speed operation in the field weakening region.

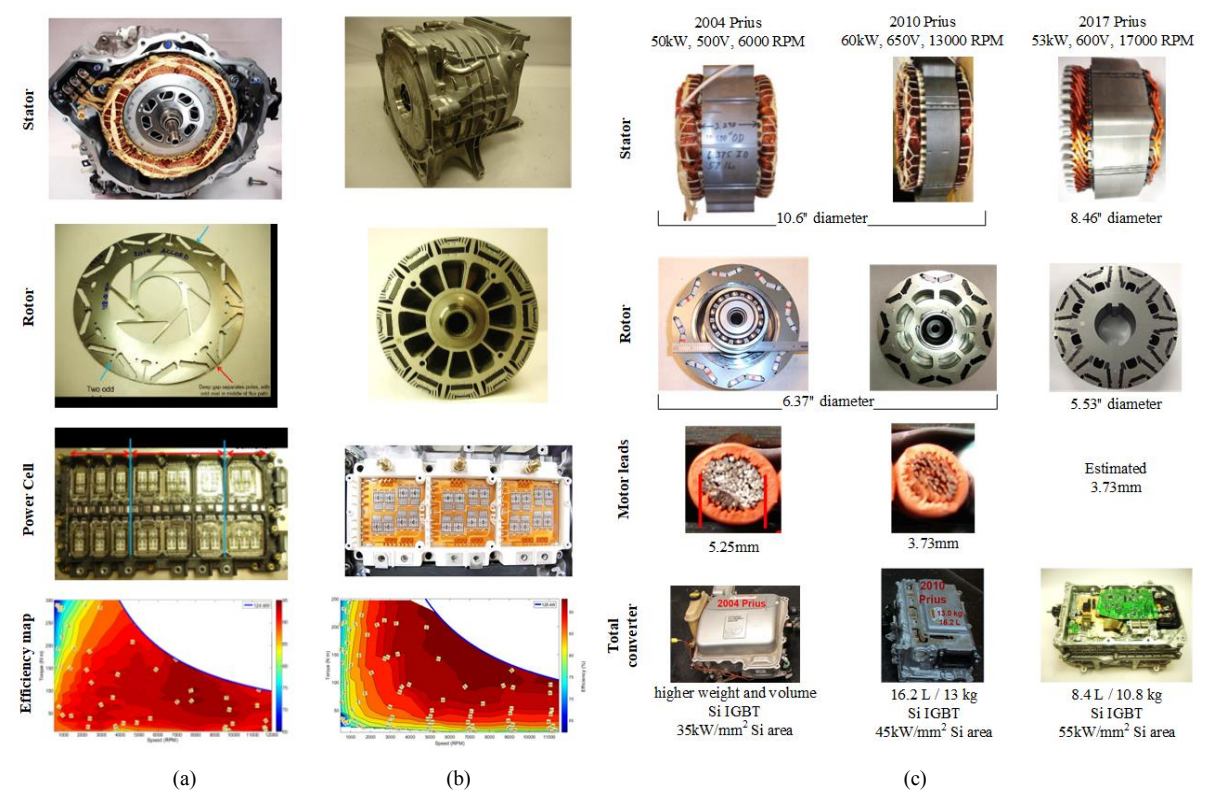


Fig. 1. From top to bottom electric motor, power cell and efficiency map for (a) 2014 Accord [3] (b) 2016 BMW i3 [3] and (c) evolution of Toyota Prius traction drive [8, 10].

#### TABLE I. EV & HEV MOTOR DRIVE PERFORMANCE [4]

Parameter	2004 Prius (50 kW)	2007 Camry (70 kW)	2008 Lexus (110 kW)	2010 Prius (60 kW)	2012 Leaf (80 kW)	2014 Accord (124 kW)	2016 BMW i3 (125 kW)	2017 Prius (53 kW)
Motor								
Peak power density (kW/L)	3.3	5.9	6.6	4.8	4.2	8.5	9.1	5.7
Peak specific power (kW/kg)	1.1	1.7	2.5	1.6	1.4	2.9	3	1.7
Inverter								
Peak power density (kW/L)	4.5(7.4)	7.4 (11.7)	10.6 (17.2)	5.9(11.1)	5.7	12.1 (18.5)	18.5	11.5 (21.7)
Peak specific power (kW/kg)	3.8(6.2)	5 (9.3)	7.7 (14.9)	6.9(16.7)	4.9	9.1 (21.7)	14.1	8.6 (19.0)
Specifications								
DC Voltage	500	650	650	650	375	700	355	600
Current (Arms)	225	282	304	170	442	300	375	~160
Number of IGBT	12	18	12	12	18	12	24	6
Total IGBT Si area (mm²)	1582.8	2165	1959.6	1312	4050	2223.12	2382	958.1

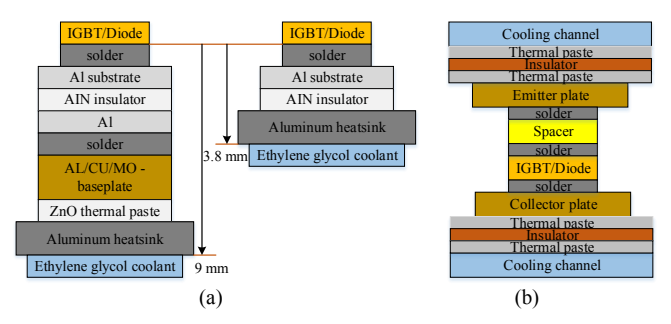


Fig. 2. Inverter cooling system (a) Prius cooling system evolution (b) 2008 Lexus LS 600h double-sided cooling.

An increase in motor speed and DC voltage led to the increment in power density by 2.2 times for 2017 Toyota Prius electric drive unit which still lags the DOE 2025 target. All the drive units studied by ORNL utilize Si IGBT-based inverters. Switching frequency used to synthesize AC voltages ranges between 1 kHz to 15 kHz with a maximum output fundamental frequency range of 400 Hz to 1 kHz [11]. Most of the system utilizes conventional planar power electronic modules where Si IGBTs are soldered directly on a substrate, and then an electrical insulator is used to isolate the power devices from the base plate, known as direct bonded copper (DBC). The conventional planar module is bolted to the heat exchanger with a thin layer of thermal interface material in between to improve heat transfer. This system is used in the 2004 Toyota Prius shown in Fig. 2(a). It can also be seen from Fig. 2(a) that 2010 Toyota Prius has reduced the layer count and increased thermal dissipation by bonding instead of bolting the power module to the heat exchanger. Innovative techniques have been utilized by other manufacturers, such as Lexus LS 600h and 2013 Toyota Camry, both of which used double sided cooling structure. This technology improves heat dissipation at the cost of complexity and overall system cost [11, 12] shown in Fig. 2(b). It is evident from the study that an increase in DC bus voltage, motor speed, and better cooling system design led to significant improvement in power density.

## III. ENABLING TECHNOLOGIES FOR COMPACT INTEGRATION

It is evident from the literature, and current ORNL study that traction drives used in the available electric vehicles are using inverters and motors in a separate casing. In this approach, the machine and the inverter require a separate cooling system, casing, and long wires. Furthermore, limited motor speed, low DC bus voltage, and Si-based semiconductors are restricting high power density solutions. To achieve DOE 2025 targets, the DC bus voltage and motor speed need to be increased. Utilization of new wide band-gap (WBG) devices, high energy density capacitor, integration of electric drive components, and better thermal management systems are needed.

## A. Integration of motor and inverter

An integrated motor drive is a physical integration of all the parts of an electric drive unit in a single casing, thus reducing volume, cost, and complexity of installation. The elimination of separate casing, bus-bars, and long wires along with sharing of the cooling system are the driving forces of increased power density for an integrated motor drive (IMD). The overall electromagnetic interference and voltage overshoot at motor terminals will also reduce due to the elimination of long cables and bus bars. A tightly integrated drive can achieve 10% - 20% better power density with reduction of manufacturing and installation cost by 30% - 40% [13]. This tight integration of motor and inverter will play a key role in traction application for electric vehicles in terms of power density and cost per unit volume.

In literature, four major types of integration techniques have been identified [14-18], shown in Fig. 3. The most common integration technique is called radial housing mount where the inverter is manufactured in a separate casing and then mounted on top of the motor casing. This type of integration has the lowest power density due to the geometry, additional casing and busbars. The other version of the radial mounting inverter system utilizes the stator outer periphery.

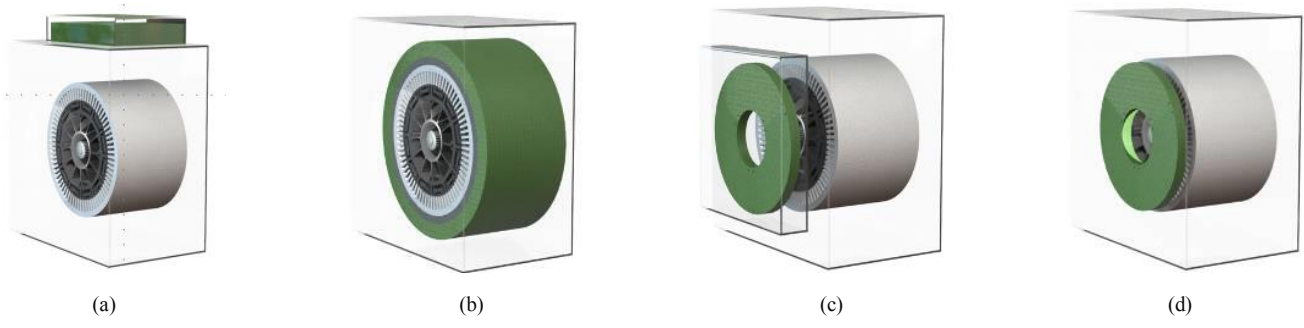


Fig. 3. Motor and inverter integration technique (a) radial housing mount (b) radial stator mount (c) axial endplate mount (d) axial stator mount.

# TABLE II. ADVANTAGES AND DISADVANTAGES OF VARIOUS INTEGRATION TECHNIQUES.

Integration techniques	Advantages	Disadvantages		
Radial housing mount	Better thermal isolation between the inverter and motor Ease of implementation and manufacturing process More space for inverter	May require a separate cooling system Achieving high power density is difficult		
Radial stator mount	Can share motor's cooling jacket Tight integration due to sharing of the cooling jacket	The outer periphery of the motor needs to have a flat surface to accommodate inverter components and PCBs		
Axial endplate mount	Endplate provides thermal isolation Ease of inverter design on top of a flat circular disk	<ul><li>A separate cold plate is required</li><li>Restricted space for inverter design</li></ul>		
Axial stator mount	Can share the same cold plate Shared cold plate will act as a thermal shield	Winding losses must conduct axially		

In this type of integration inverter and the motor share the same cooling system as shown in Fig. 3(b). The other two integration techniques mentioned in the literature are axially mounted inverter, where the inverter is either directly connected to the endplate or it is connected in between the stator lamination and endplate. The latter suffers from an extreme environment as the inverter is mounted next to the major heat source (stator winding). The advantages and disadvantages of the identified integration techniques are presented in Table II. It is evident from the literature that the integration of motor and inverter will reduce the component count of a traction drive system thus overall system cost and volume will reduce [13].

#### B. Power module

Power semiconductor modules used in the inverter are responsible for electric power transfer between the source and the load. The efficiency of such systems has become quite high due to recent advancements in silicon-based power semiconductor devices. The efficiency numbers are usually above 90% for systems rated more than 1 kW output power. With the advancements in wide-bandgap (WBG) based power semiconductor devices such as SiC MOSFET and GaN HEMT, efficiency figures above 98% have been reported in the literature [19]. However, even with very highefficiency figures, a significant amount of power is dissipated in a small area. This is due to increased power demand from the electrical load, increased power density of power modules, and reduced chip size with the introduction of wide-bandgap devices [20]. Therefore, the performance of the materials used for packaging, integration of power modules, and design of thermal management systems have become the focal points of next-generation power electronic systems, especially in application domains such as electric vehicles.

Furthermore, WBG devices operate at much higher switching speed, and the impact of parasitic components (e.g. parasitic inductance and capacitance) introduced by the module design must be minimized. This is required for optimizing system efficiency and maximizing benefits of using high-speed switching devices. The illustration of a conventional power module cross section is shown in Fig. 4, where various components of the structure are highlighted. The structure is composed of different materials such as aluminum for bond wire, copper for the electrical terminal, ceramic-based direct bonded copper substrate, etc. This multi-layer, multi-material based structure has limited heat extraction capability. The usage of bond wire based interconnects between power semiconductor dies and terminals also increase parasitic inductance. Furthermore, certain layers in the structure shown in Fig. 4 are subject to high mechanical stress. This is due to different coefficients of thermal expansion (CTE) between layers, thus leading to limited lifetime and early failures caused by thermal stress [21].

SiC MOSFET based power modules are offered by major device and module manufacturers such as Infineon, CREE, ROHM, and Semikron in various circuit topologies. Operating temperatures of these modules are limited to 150-175°C, and the structure is based on the illustration in Fig. 4. However, the Infineon Easy 1B and Semikron Mini Skiip modules do not have a base plate to improve the thermal performance and easy assembly with pin type terminals and screw mounting options [10]. All these packages are designed for Si IGBT devices and used for high maturity of

the design, low cost, and easy adoption by design engineers. However, they do not meet the needs for high-performance power packaging for WBG devices due to high parasitic inductance and high thermal requirements. The high parasitic inductance will cause excessive voltage stress and ringing across the power devices during high-speed switching transitions and will result in high switching losses. The high thermal requirement of the module to keep the devices at the desired junction temperature for the rated power value. This results in a low power density system due to the large cooling system requirement. The commercially available modules have parasitic inductance values varying between 15nH – 20nH, which is not suitable for WBG devices [10].

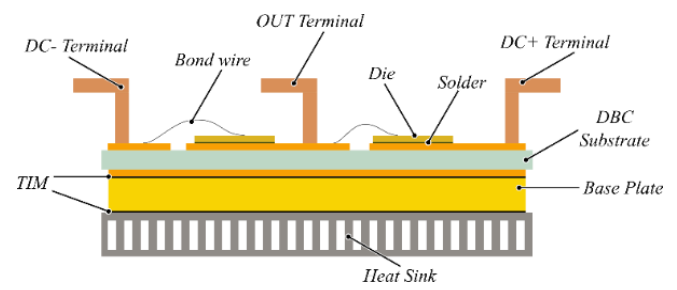


Fig. 4. Illustration of a conventional power module.

To overcome the challenges of the commercial power modules from power module manufacturers, several highpower density power electronics packaging architectures have been proposed by academia and industry.

GE Global Research has proposed an embedded power module structure approach called "GE Power Overlay (POL)". The design is based on replacing the wire bond interconnects in the conventional solution with a planar interconnect [22]. This solution provides low and matched electrical parasitic that leads to low inductance, low resistance and therefore high-power efficiency. It can be applied in large panel process and can be used to integrate power and signal dies in the same package for high power density. Siemens has also proposed an embedded power module structure called "Siemens SiPLIT". The Siemens module is based on soldering of the power dies on a direct bonded copper (DBC) substrate, and low-profile copperbased interconnects acting as high-density interconnects [23]. Delphi developed a bespoke double-sided planar module for SiC devices based on paralleled SiC MOSFET dies sandwiched between two DBC substrates [24]. Unlike the other solutions presented earlier, this structure allows double-sided cooling but accommodates only one switch (five dies in parallel per switch) per module. Major drawbacks of such a design are the asymmetric layout of the paralleled switches which may lead to unbalanced current sharing during switching transitions and external commutation loop inductance of the switching cell. This phenomenon will be dominated by the series connection of Viper modules to form a half bridge cell [24].

Oak Ridge National Laboratory (ORNL) has also developed a double-sided power module architecture targeted for wide-bandgap devices [25, 26]. The planar-bond-all (PBA) structure of the proposed architecture is shown in Fig. 5. The package features sandwiching of power semiconductor switches between two direct bond copper (DBC) substrates and using copper shims to eliminate wire bonds for power loop. Two cold plates (coolers) are directly bonded to the outside of these substrates, allowing double sided, integrated cooling. The enclosed area of the main current loop in this new interconnection configuration is

reduced dramatically with the replacement of wire bonds with copper shims. The elimination of wire bonds leads to a significant reduction in electrically parasitic inductance and resistance allowing for full utilization of WBG switches.

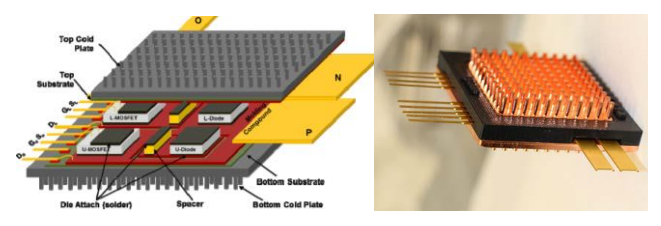


Fig. 5. ORNL PBA double-sided cooling structure [26].

The ORNL PBA module has three times less loop inductance (1.5 nH) in comparison to commercial solutions and provides 50% higher current density at 120°C junction temperature [25]. The wide-bandgap devices demand these drastic performance enhancements from the module packaging to perform the true potential of material characteristics. High performance of the module is one of the enablers to achieve high power density in an integrated traction drive system.

## C. Inverter topology

Inverters are used in the electric traction drive systems to supply power to the motor. There are various types of topologies available; among them, manufacturers have adopted two-level voltage source inverter (VSI), due to simpler design, robustness and easy controllability. The two-level inverter switches must block the full DC bus voltage; thus switching losses are higher compared to multilevel converters. The output leg voltage swings between zero and full DC voltage; thus dv/dt is higher as well. This inverter can be replaced with multilevel inverters to achieve low loss and low dv/dt. A three-level neutral point clamped (NPC) can be a potential candidate for higher frequency operation with reduced dv/dt [27], shown in Fig. 6(b).

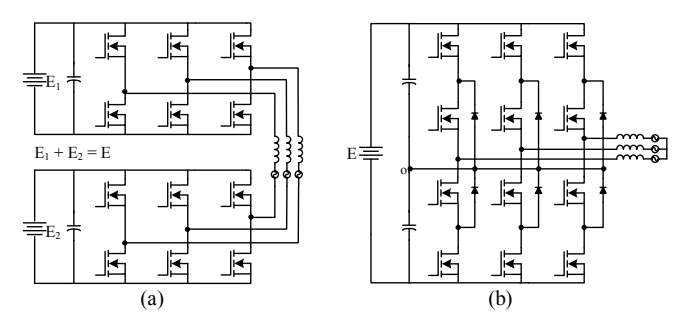


Fig. 6. Three-level inverter topology (a) dual inverter with equal voltage ratio (b) three-level NPC inverter.

To add redundancy one can also utilize an open-end winding configuration [28, 29]. This inverter topology uses dual two-level inverters and can achieve three level output voltage, shown in Fig. 6(a). The dual inverter is also operational with reduced power under open or short circuit fault. However, the inverters described above will utilize more switches than conventional two-level inverters and more gate drivers will be needed. Control complexity will also increase. Overall, these approaches might not help achieve the cost and power density targets.

To reach DOE 2025 target of 100kW/L a different approach is taken. Instead of directly looking into loss and volume reduction of an inverter, an approach to reduce DC

bus capacitor volume is considered for inverter volume optimization. The standard voltage source inverter (VSI) generates large ripple currents in the DC link and thus requires a large DC bus filter capacitor, which may take up to 20% of the inverter volume. The segmented inverter was proposed in [30] that can significantly reduce the dc bus ripple current and the capacitance. The process of changing a stand VSI based drive to the segmented traction drive system is shown in Fig. 7. The inverter switches in the power module and stator windings in the motor are separated into two sets of switches (indicated in red and blue in the figure) and windings  $(a_1, b_1, c_1)$  and  $(a_2, b_2, c_2)$ . Further, each phase group of the stator windings  $(a_1, a_2)$ ,  $(b_1, b_2)$ , and  $(c_1, c_2)$  can be collocated in the same stator slots or displaced in different regions for a multipole motor. Each group of switches (red or blue) is connected as a three-phase inverter bridge and connects to one set of the motor stator windings, forming an independent drive unit. Because switches in most high power inverter modules are comprised of multiple switches and diode dies connected in parallel, only minor modifications to the switch configuration are required to form a segmented inverter.

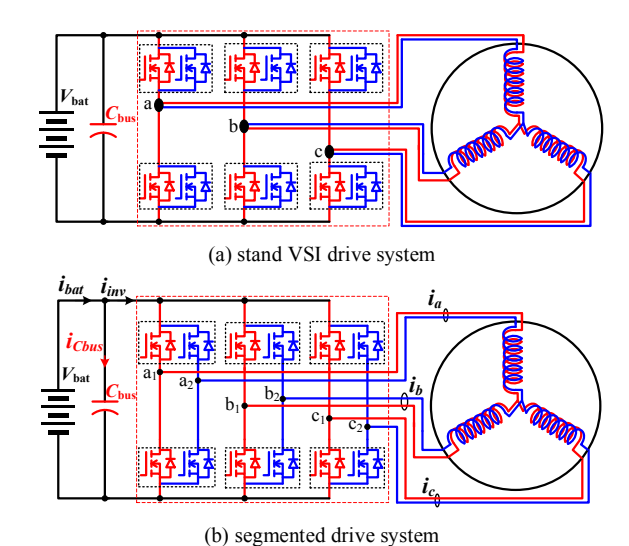


Fig. 7. Changing from a standard two level VSI drive to the segmented drive system.

The timing of the turn-on and turn-off of the corresponding switches in the two independent drive units is controlled with interleaved switching for carrier-based PWM methods. No changes are needed in the implementation of control of the motor except the modifications in the PWM control of the switches in the inverter. To control the motor speed or torque, two of the combined three phase motor currents,  $i_a = (i_{a1} + i_{a2})$ ,  $i_b = (i_{b1} + i_{b2})$ , and  $i_c = (i_{c1} + i_{c2})$ , along with the motor speed or rotor position are sensed and fed to a chosen motor control scheme, which is typically based on the field orientation control. Therefore, no additional current sensors are required, compared to the standard electric drive.

Fig.8 plots a comparison of measured capacitor ripple currents at various levels of load torque and motor speed for the standard and segmented inverters in an induction motor drive. The capacitor ripple currents are normalized against the rated motor current of 37.5 Arms. The segmented inverter offers a significant reduction of capacitor ripple current, in the range of 55% to 75%, at the rated torque; 50% to 70% at 75 % of rated torque; and 50% to 60% at 50% of rated torque. It is also worth noting that the maximum ripple current with the standard VSI approaches the rated motor current.

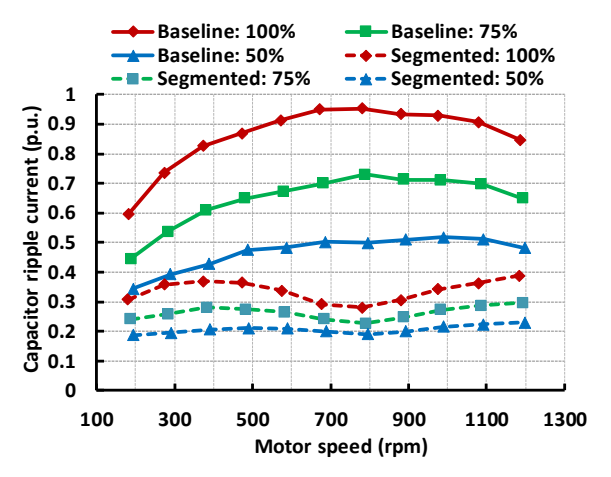


Fig. 8. Comparison of normalized capacitor ripple current vs. motor speed at load torque of 100%, 75%, and 50% of rated torque of 91 Nm with a rated current of 37.5 Arms.

It is evident from the simulation results that the usage of the segmented inverter will reduce capacitor ripple current thus the capacitor volume will reduce without increasing the module volume. This inverter can be used to drive a traction motor and can achieve much higher power density than a two-level or the aforementioned multilevel inverters.

#### D. Traction motor

Electric motors convert the electric energy into rotational energy that is transferred to the wheels to propel the vehicle. Many types of electric motors have been used by EV manufacturers, and each of them has their advantages and disadvantages regarding compactness, efficiency, speed range, and reliability. Three main types of motors are currently used by major EV manufacturers: induction motors (IM), wound rotor synchronous motor (WRSM) and permanent magnet motors (PMM).

Induction motor technology is an old, and thereby very mature technology. Induction motors are cost-effective, robust and are very easy to control. This explains why they are widely used in industrial applications. Nevertheless, their low power factor results in a higher rated inverter. Also, because of the eddy current loss in the rotor bars, the efficiency is lower compared to the synchronous counterparts. The rotor of an induction motor requires cooling, which can be challenging for high-speed operation. These motors have lower power density than WRSM and PMMs as well as has limited constant power range. Due to these reasons, few passenger EV manufacturers are using induction traction motors. As an example, Audi uses a threephase IM for its e-tron EV, coupled to the axle through a gearbox [31] and Tesla uses induction motors in Model S and X vehicles. Its stator is cooled through a water cooling jacket, and the rotor features an internal water cooling structure to cool down the rotor.

Wound rotor synchronous motor is being used by Renault in its Zoe EV [32]. In addition to being non-rare-earth, the WRSM has the advantage of a higher power factor over IMs, and the adjustability of the rotor field over PMMs. In [33], WRSM option has been shown to be as power dense as the PMM counterpart. However, because of the copper losses in the rotor, WRSM has lower efficiency and requires rotor cooling. Furthermore, an additional converter is needed to supply the rotor winding, adding complexity to the control algorithm. The main disadvantage of WRSM is the use of slip ring and brush contacts to power the rotor winding. This

is an important reliability issue, especially for high-speed operation. To solve these issues, contactless rotary transformer-based rotor excitation systems were proposed in [34] and [33]. WRSM option can be a good compromise between power density, efficiency, and cost.

Permanent magnet motors are the most popular choice to maximize both compactness and efficiency. PMMs are currently used in the most popular passenger EVs such as Tesla Model 3, Toyota Prius, Nissan Leaf, BMW-i3 and Chevy Bolt. In fact, PMM has the highest power density, and the best efficiency since the production of the rotor field does not involve any loss. Most of the PMMs used in EV traction are Internal Permanent Magnet (IPM) rotors, shown in Fig.9. IPM rotors have magnetic saliency that produces an additional reluctance torque and further increases the power density. Most of IPM traction motors use distributed winding, shown in Fig. 10(a). There are two main reasons for using distributed winding: 1) because of the low harmonic content of its magnetomotive force (MMF) which helps minimize stator iron loss and rotor loss; 2) to take full advantage of the reluctance torque.





Fig. 9. Different IPM rotor geometries: (a) BMW-i3 rotor [3] (b) Toyota Prius rotor [4].





Fig. 10. Stator winding: (a) distributed winding [4]; (b) concentrated winding with short end winding [11].

The main disadvantage of the PMM option is the cost of heavy rare-earth (HRE) materials used in the permanent magnets. Heavy rare-earth materials such as Dysprosium (Dy) and Terbium (Tb) have seen price volatility and concerns over the reliability of their supply. For these reasons, global effort in developing heavy rare-earth-free permanent magnet materials is underway. In the US, power density goal of 50kW/L and a speed range up to 20,000 rpm is set for non-heavy rare-earth traction motors by the DOE 2025 roadmap. PMMs using HRE-free magnet materials are the most promising electric motor candidates with the potential to achieve such aggressive targets. However, since the elimination of HRE generally leads to a reduction in coercivity, special attention should be paid during the design to ensure the rotor is resistant to demagnetization.

One way to reduce the motor volume is through a design with a higher number of poles. This will, however, increase the frequency of operation and will require iron loss and AC loss mitigation techniques along with cooling challenges. A modular concentrated winding technology is shown in Fig.10(b). This winding technology can reduce the end winding length and thereby the motor volume. However, because of the rich harmonic content of its MMF, a concentrated winding will generate more stator and rotor iron losses as well as more eddy current losses in the permanent magnets. Hence, active rotor cooling will be required.

Finally, the development of new low-loss lamination, as well as high coercivity HRE-free permanent magnet materials will be key to achieving the DOE 2025 power density and performance target.

## E. Capacitor technology

DC bus capacitor imposes an obstruction to meet highpower density demand in VSI employed in electric traction drives. The main purpose of the DC bus capacitor is to decouple the load from the DC supply unit thus the capacitor absorbs a large ripple current and retains the voltage transients due to inverter switching action. These capacitors use substantial space, about 20% of an inverter thus better capacitor technology with proper sizing is required. There are several capacitor technologies available in the market most commonly used ones are electrolytic capacitors, ceramic capacitors, and film capacitors. Among the three of them, the film capacitor technology is widely used as DC bus capacitor for EV traction drive applications. Though these capacitors have low capacitances per unit volume than electrolytic capacitors, they have gained interest due to their reliability, high current capability, and lower equivalent series resistance (ESR).

The other candidate for DC bus capacitor is the ceramic capacitor, these types of capacitors use ceramic dielectric and have a very high dielectric constant. These capacitors can be constructed using a single layer capacitor for small capacitance or can be constructed by stacking multiples of them together to form multilayer ceramic capacitors (MLCC). The ceramic capacitor has a much higher RMS current rating per unit volume, can withstand higher temperature, and has a much higher capacitance density. A ferromagnetic material-based dielectric is used to form the capacitor. The most common dielectric used in MLCC is called Barium Titanate (BaTio3) this is a class II dielectric material [35]. The parameters of class II dielectric material are highly temperature dependent.

The capacitance of the MLCC decreases rapidly with DC bias voltage. There are reliability issues associated with ceramic capacitors due to the rigid dielectric material that can crack due to mechanical and thermal stress [36, 37]. Because of these reasons, the ceramic capacitors are not gaining popularity to use as a DC bus capacitor for traction motor drive for EV application.

There is another type of ceramic capacitor available in the market named CeraLink capacitor, a trademark of TDK. This capacitor has inherited all the advantages of MLCC capacitors and has increased reliability by utilizing a series connection of two MLCC geometries in one component, shown in Fig. 11. These capacitors use an antiferroelectric material as dielectric thus their capacitance increases with DC bias. Moreover, the dielectric characteristics do not change much with the change in temperature [38].

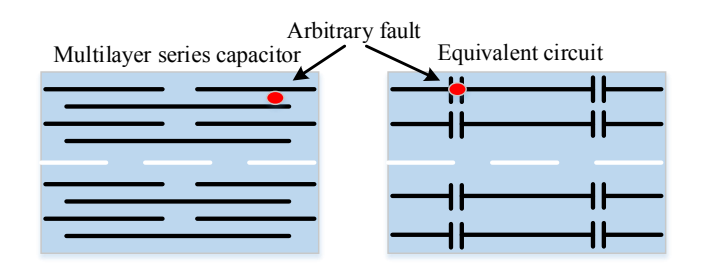


Fig. 11. Multilayer series connected capacitor used in CeraLink capacitor technology.

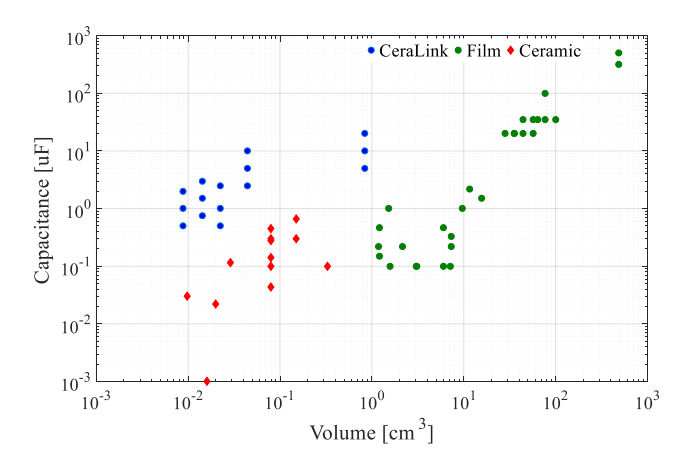


Fig. 12. Capacitance density of three capacitor technologies.

To realize high energy density capacitors, 55 samples of Ceramic, CeraLink, and Film capacitors were chosen and their capacitances per unit volume were plotted in Fig. 12. These capacitors are off the shelf capacitors available in the market to purchase and have a voltage range between 450 V – 1000 V. It is evident from Fig. 12. that the CeraLink capacitors have the highest capacitance density and can be used to optimize the volume of traction drive inverters.

# IV. CONCLUSION

This paper provides a brief review of the commercially available electric drive system for EV traction application. The design trends of commercially available electric drive units have been highlighted. It is evident from the review that the modern EV traction drives are becoming more efficient and power dense, but still lagging the DOE 2025 power density target. To increase the power density of a traction drive several aspects of an electric drive unit has been addressed in this paper. The integration of motor and inverter along with smaller power dense module design incorporating WBG devices can significantly bring down the volume of the overall system.

Furthermore, a segmented inverter topology is discussed to reduce DC bus capacitor current stress along with identification of energy-dense capacitor technology to reduce passive component volume. Finally, motor design aspects are discussed to manufacture smaller volume motors. Utilizing these mentioned technologies for traction application can help to achieve a compact electric traction drive for EV application.

#### ACKNOWLEDGMENT

This material is based upon work supported by the U.S. Department of Energy, Office of Energy Efficiency and Renewable Energy, Vehicle Technologies Office under

contract number DE-AC05-00OR22725. The authors would like to thank the U.S. Department of Energy's Susan Rogers for her financial support.

#### REFERENCES

- [1] L. Ulrich, "Top 10 Tech cars: 2018 [Top 10 Tech Cars]," *IEEE Spectrum*, vol. 55, no. 4, pp. 30-41, 2018,doi: 10.1109/MSPEC.2018.8322044.
- [2] "Electrical and Electronics Technical Team Roadmap," [Online]. Available: https://www.energy.gov/sites/prod/files/2017/11/f39/EETT%20Roadmap%2010-27-17.pdf, Accessed on: Dec. 12, 2018.
- [3] T. Burress. "Benchmarking EV and HEV Technologies," [Online]. Available: https://www.energy.gov/sites/prod/files/2016/06/f32/edt006\_burress\_2016\_o\_web.pdf, Accessed on: Dec. 12, 2018.
- [4] T. Burress. "Electrical Performance, Reliability Analysis, and Characterization," [Online]. Available: https://www.energy.gov/sites/prod/files/2017/06/f34/edt087\_burress\_2017\_o.pdf, Accessed on: Dec. 12, 2018.
- [5] T. Burress. "Benchmarking of Competitive Technologies," [Online]. Available: https://www.energy.gov/sites/prod/files/2014/03/f12/ape006\_burre ss\_2010\_o.pdf, Accessed on: Dec. 12, 2018.
- [6] C. W. Ayers, "Evaluation of 2004 Toyota Prius Hybrid Electric Drive System Interim Report," *United States: N. p.,*, 2004, Web.,doi: 10.2172/885776.
- [7] T. Burress. "Benchmarking State-of-the-Art Technologies," [Online]. Available: https://www.energy.gov/sites/prod/files/2014/03/f13/ape006\_burre ss\_2013\_o.pdf, Accessed on: Dec. 12, 2018.
- [8] T. Burress. "Benchmarking of Competitive Technologies" [Online]. Available: https://www.energy.gov/sites/prod/files/2014/03/f10/ape006\_burress\_2011\_o.pdf, Accessed on: Dec. 12, 2018.
- [9] T. A. Burress, Campbell, Steven L, Coomer, Chester, Ayers, Curtis William, Wereszczak, Andrew A, Cunningham, Joseph Philip, Marlino, Laura D, Seiber, Larry Eugene, and Lin, Hua-Tay, "Evaluation of the 2010 Toyota Prius Hybrid Synergy Drive System," *United States: N. p.*, , 2011, Web.,doi: 10.2172/1007833.
- [10] C. Chen, F. Luo, and Y. Kang, "A review of SiC power module packaging: Layout, material system and integration," *CPSS Transactions on Power Electronics and Applications*, vol. 2, no. 3, pp. 170-186, 2017,doi: 10.24295/CPSSTPEA.2017.00017.
- [11] T. Burress and S. Campbell, "Benchmarking EV and HEV power electronics and electric machines," in 2013 IEEE Transportation Electrification Conference and Expo (ITEC), 2013, pp. 1-6.
- [12] T. A. Burress, Coomer, C.L., Campbell, S.L., Wereszczak, A.A., Cunningham, J.P., Marlino, L.D., Seiber, L.E., and Lin, H.T., "Evaluation of the 2008 Lexus LS 600H Hybrid Synergy Drive System," *United States: N. p.*, , 2009, Web.,doi: 10.2172/947393.
- [13] F. M. D. Throne, R. Marguire, D. Arens. "Integrated Motor/Drive technology with Rockwell connectivity," [Online]. Available: http://www.cmafh.com/enewsletter/PDFs/IntegratedMotorDrives.p df, Accessed on: Dec. 14, 2018.
- [14] R. Abebe *et al.*, "Integrated motor drives: state of the art and future trends," *IET Electric Power Applications*, vol. 10, no. 8, pp. 757-771, 2016,doi: 10.1049/iet-epa.2015.0506.
- [15] W. Lee, S. Li, D. Han, B. Sarlioglu, T. A. Minav, and M. Pietola, "A Review of Integrated Motor Drive and Wide-Bandgap Power Electronics for High-Performance Electro-Hydrostatic Actuators," *IEEE Transactions on Transportation Electrification*, vol. 4, no. 3, pp. 684-693, 2018,doi: 10.1109/TTE.2018.2853994.
- [16] J. Wang, Y. Li, and Y. Han, "Integrated Modular Motor Drive Design With GaN Power FETs," *IEEE Transactions on Industry Applications*, vol. 51, no. 4, pp. 3198-3207, 2015,doi: 10.1109/TIA.2015.2413380.
- [17] M. Nikouie, H. Zhang, O. Wallmark, and H. Nee, "A highly integrated electric drive system for tomorrow's EVs and HEVs," in 2017 IEEE Southern Power Electronics Conference (SPEC), 2017, pp. 1-5.
- [18] N. R. Brown, T. M. Jahns, and R. D. Lorenz, "Power Converter Design for an Integrated Modular Motor Drive," in 2007 IEEE Industry Applications Annual Meeting, 2007, pp. 1322-1328.
- [19] E. Gurpinar and A. Castellazzi, "Single-Phase T-Type Inverter Performance Benchmark Using Si IGBTs, SiC MOSFETs, and GaN HEMTs," *IEEE Transactions on Power Electronics*, vol. 31, no. 10, pp. 7148-7160, 2016,doi: 10.1109/TPEL.2015.2506400.

- [20] K. Suganuma, Wide Bandgap Power Semiconductor Packaging: Materials, Components, and Reliability. Elsevier Science, 2018.
- [21] A. M. Aliyu and A. Castellazzi, "Prognostic System for Power Modules in Converter Systems Using Structure Function," *IEEE Transactions on Power Electronics*, vol. 33, no. 1, pp. 595-605, 2018,doi: 10.1109/TPEL.2017.2672823.
- [22] L. Stevanovic, "Packaging Challenges and Solutions for Silicon Carbide Power Electronics," presented at the ECTC Panel Session: Power Electronics – A Booming Market, San Diego, 2012.
- [23] K. Weidner, M. Kaspar, and N. Seliger, "Planar Interconnect Technology for Power Module System Integration," in 2012 7th International Conference on Integrated Power Electronics Systems (CIPS), 2012, pp. 1-5.
- [24] M. B. Hayes. "650V Silicon Carbide Integrated Power Module for Automotive Inverters," [Online]. Available: https://www.energy.gov/sites/prod/files/2018/06/f52/elt083\_hayes \_2018\_o\_.pdf, Accessed on: April. 15, 2019.
- [25] Z. Liang, P. Ning, and F. Wang, "Development of Advanced All-SiC Power Modules," *IEEE Transactions on Power Electronics*, vol. 29, no. 5, pp. 2289-2295, 2014,doi: 10.1109/TPEL.2013.2289395.
- [26] Z. Liang, "Integrated double sided cooling packaging of planar SiC power modules," in 2015 IEEE Energy Conversion Congress and Exposition (ECCE), 2015, pp. 4907-4912.
- [27] R. Vargas, P. Cortes, U. Ammann, J. Rodriguez, and J. Pontt, "Predictive Control of a Three-Phase Neutral-Point-Clamped Inverter," *Industrial Electronics, IEEE Transactions on*, vol. 54, no. 5, pp. 2697-2705, 2007, doi: 10.1109/TIE.2007.899854.
- [28] S. Chowdhury, P. Wheeler, Z. Huang, M. Rivera, and C. Gerada, "Fixed switching frequency predictive control of an asymmetric source dual inverter system with a floating bridge for multilevel operation," *IET Power Electronics*, vol. 12, no. 3, pp. 450-457, 2019,doi: 10.1049/iet-pel.2018.5395.
- [29] B. A. Welchko, "A double-ended inverter system for the combined propulsion and energy management functions in hybrid vehicles with energy storage," in 31st Annual Conference of IEEE Industrial Electronics Society, 2005. IECON 2005., 2005, p. 6 pp.
- [30] G. Su and L. Tang, "A segmented traction drive system with a small dc bus capacitor," in 2012 IEEE Energy Conversion Congress and Exposition (ECCE), 2012, pp. 2847-2853.
- [31] "Inside Audi's e-tron Electric Motor Design," [Online]. Available: https://e-racing365.com/features/videos/inside-audi-e-trons-electric-motor-design/, Accessed on: April, 15, 2019.
- [32] "Renault boosts ZÕE EV's range by almost 15% to 149 miles with new motor unit," [Online]. Available: https://www.greencarcongress.com/2015/03/20150304-zoe.html, Accessed on: April, 15, 2019.
- [33] C. Stancu, T. Ward, K. M. Rahman, R. Dawsey, and P. Savagian, "Separately Excited Synchronous Motor With Rotary Transformer for Hybrid Vehicle Application," *IEEE Transactions on Industry Applications*, vol. 54, no. 1, pp. 223-232, 2018,doi: 10.1109/TIA.2017.2757019.
- [34] T. Raminosoa and R. Wiles, "Contactless Rotor Excitation for Traction Motors," in 2018 IEEE Energy Conversion Congress and Exposition (ECCE), 2018, pp. 6448-6453.
- [35] R. U. A. Shaikh, A. Saeed, and R. Kumar, "Review on present and future integration techniques for capacitors in motor drives," in 2018 International Conference on Computing, Mathematics and Engineering Technologies (iCoMET), 2018, pp. 1-8.
- [36] T. Kobayashi, H. Ariyoshi, and A. Masuda, "Reliability Evaluation and Failure Analysis for Multilayer Ceramic Chip Capacitors," *IEEE Transactions on Components, Hybrids, and Manufacturing Technology*, vol. 1, no. 3, pp. 316-324, 1978,doi: 10.1109/TCHMT.1978.1135275.
- [37] H. Wang, C. Liang, T. Lu, H. Xiao, and W. Tian, "Failure analysis of multilayer ceramic capacitor board level interconnect caused by monotonic bending stress," in 2016 11th International Conference on Reliability, Maintainability and Safety (ICRMS), 2016, pp. 1-5.
- [38] D. Neumayr, D. Bortis, J. W. Kolar, M. Koini, and J. Konrad, "Comprehensive large-signal performance analysis of ceramic capacitors for power pulsation buffers," in 2016 IEEE 17th Workshop on Control and Modeling for Power Electronics (COMPEL), 2016, pp. 1-8.